

The density profile of equilibrium and non-equilibrium dark matter halos

Y.P. Jing

Research Center for the Early Universe, School of Science, University of Tokyo, Bunkyo-ku,
Tokyo 113-0033, Japan
e-mail: jing@utaphp2.phys.s.u-tokyo.ac.jp

ABSTRACT

We study the diversity of the density profiles of dark matter halos based on a large set of high-resolution cosmological simulations of 256^3 particles. The cosmological models include four scale-free models and three representative cold dark matter models. The simulations have good force resolution. In each cosmological model, there are about 400 massive halos which have more than 10^4 particles within the virial radius. Our unbiased selection of all massive halos enables us to quantify how well the bulk of dark matter halos can be described by the Navarro, Frenk & White (NFW) profile which was established for equilibrium halos. We find that about seventy percent of the halos can be fitted by the NFW profile with a fitting residual dvi_{\max} less than 0.3 in $\Omega_0 = 1$ universes. This percentage is higher in the low-density cosmological models of $\Omega_0 = 0.3$. The rest of the halos exhibits larger deviation from the NFW profile for more significant internal substructures. There is a considerable amount of variation in the density profile even among the halos which can be fitted by the NFW profile (i.e. $dvi_{\max} < 0.30$). The distribution of the profile parameter, the concentration c , can be described well by a lognormal function with the mean value \bar{c} slightly smaller (15%) than the NFW result and the dispersion σ_c in $\ln c$ about 0.25. More virialized halos with $dvi_{\max} < 0.15$ have the mean value \bar{c} in better agreement with the NFW result and their dispersion σ_c is also slightly smaller (about 0.2). Our results can alleviate some of the conflicts found recently between the theoretical NFW profile and observational results. Implications for theoretical and observational studies of galaxy formation are discussed.

Subject headings: galaxies: formation — large-scale structure of universe — cosmology: theory — dark matter

1. Introduction

In their recent series of papers, Navarro, Frenk, & White (NFW; 1995, 1996, 1997) investigated the density profile $\rho(r)$ for Dark Matter (DM) halos in cosmological models of hierarchical clustering. They concluded that the density profile has a universal form,

$$\rho_{NFW}(r) \propto \frac{1}{r(r+r_s)^2} = \frac{1}{r_{200}^3 x(x+1/c)^2}, \quad (1)$$

where r_s is the core radius, r_{200} is the virial radius within which the mean density is 200 times the critical density ρ_{crit} , x is the radius scaled with r_{200} , and $c \equiv r_{200}/r_s$ is the concentration parameter. For a given virial mass M_{200} , its virial radius r_{200} is fixed [given by $(3M_{200}/800\pi\rho_{\text{crit}})^{1/3}$] and the profile has only one free parameter c . Their simulation results show that c depends only on the halo mass for a given cosmological model. Furthermore they proposed a recipe based on the Press-Schechter theories with which one can predict c very accurately for any hierarchical model. All these results have significant impact on theoretical and observational studies of galaxy formation. The density profile has been widely used for modeling galaxy formation (e.g. Dalcanton, Spergel & Summers 1997, Mo Mao & White 1998, Mao & Mo 1998, van den Bosch 1998) and for interpreting and confronting various observational data (e.g., Persic Salucci & Stel 1996, Carlberg et al. 1997a,b, Makino Sasaki & Suto 1998, Tyson et al. 1998, MCGaugh & De Blok 1998, Navarro 1998).

While it is truly important to emphasize the universality of the density profile as NFW already did, our present work will focus on another important aspect of the density profile: diversity. The halos NFW studied are intentionally selected to be at the equilibrium state. NFW picked up the dark matter halos which *look in equilibrium* from (lower-resolution) cosmological simulations and resimulated them at high resolution using fine and coarse particles. They checked the ratio of the kinetic energy to the potential energy for each halo from redshift $z = 0.1$ to the final epoch ($z = 0$) and measured the density profile at the epoch ($0.1 \geq z \geq 0$) when the halo is closest to equilibrium according to the virial theorem. With this procedure, NFW attempted to avoid non-equilibrium DM halos. This selection procedure however left two important questions to be answered. First, how much fraction of the DM halos can be described by the NFW profile? This question is closely related to the well-known fact that quite a fraction of DM halos has a significant amount of substructures; strictly speaking, very few DM halos are in equilibrium (e.g. Jing et al. 1995; Thomas et al. 1998). Second, even for the halos which can be fitted by the NFW profile, what is the distribution of the profile parameter c ? Answering both questions would be of vital importance for the theoretical modeling and the observational interpretation based on the NFW profile.

To answer these questions, one needs a good sample of DM halos. The sample must be large and well-defined, and the individual halos must be well-resolved. In this paper, we use a large set of high-resolution cosmological simulations of 256^3 particles (Jing & Suto 1998; Jing 1998a) to study these problems. The simulations were generated with our Particle-Particle/Particle-Mesh (P³M) code which has high force-resolution. Four scale-free models with $P(k) \propto k^n$ ($n = -0.5, -1, -1.5$, and -2.0) and three representative CDM models are simulated. In each model, there is a total of a few hundred massive halos with more than 10^4 particles within the virial radius r_{200} . Both the force and the mass resolutions of our halos are comparable to those of NFW. But our unbiased selection of all halos and the large number of the halos enable us to answer the questions NFW left.

Our results will show that the goodness of the NFW profile fitting depends on if the halo is in equilibrium. About 15 to 40 percent of DM halos, depending on the density parameter Ω_0 , cannot be fitted well by the NFW profile because of a significant amount of substructures. The rest of halos which are more close to equilibrium can be described quite well by the NFW profile, with the fitting residual less than 30 percent. For these halos which can be fitted by the NFW profiles, there is a considerable dispersion in the density profiles even for the same mass M_{200} in the same cosmological model. The dispersion is characterized by the distribution of the concentration parameter c . We will, for the first time, show that the distribution of c can be well described by a lognormal function, with the mean value of c very close to the NFW result and the scatter σ_c in $\ln c$ about 0.25. Our result therefore essentially confirms the conclusion of NFW, but significantly extends the study of the density profiles to a wider range of halos with different physical properties. We will discuss the implications of our result for theoretical and observational studies in Sect. 4. A summary of these results already appeared in the conference proceedings *Evolution of Large-scale Structure* at Garching, 1998 (Jing 1998b).

In the next section (§2) we will discuss our simulations. Our results for the density profiles will be presented in §3. We will summarize our results and discuss their implications for the studies of galaxy formation in §4.

2. Simulations

We use a set of high-resolution simulations of 256^3 particles which were generated with our vectorized P³M code on the supercomputer Fujitsu VPP300/16R at the National Astronomical Observatory of Japan. The simulations were evolved typically by 1000 steps, with a force resolution ϵ (ϵ is the force softening of the Plummer form) about 2×10^{-4} of the simulation box size. We will use only the final output of each simulation for the present

study. The simulations cover three representative Cold Dark Matter (CDM) models and four Scale-Free (SF) models of hierarchical clustering. The CDM models are specified with the density parameter Ω_0 , the cosmological constant λ_0 , the shape Γ and the normalization σ_8 of the linear power spectrum $P(k)$. The SF models assume an Einstein–de Sitter universe (i.e. $\Omega_0 = 1$ and $\lambda_0 = 0$) and a power-law $P(k) \propto k^n$ for the linear density power spectrum. The amplitude of $P(k)$ for the SF models are set by the non-linear mass M_* at which the rms linear density fluctuation $\sigma(M_*)$ is 1.68. Table 1 summarizes the model parameters. The simulations have been used to study the theoretical significance of the strong clustering of high-redshift galaxies (Steidel et al. 1998) by Jing & Suto (1998) and to derive the accurate fitting formula for the halo clustering by the author (Jing 1998a; 1999). We refer readers to these papers for complementary information about these simulations.

3. The distribution of density profiles

We select DM halos using the Friends-of-Friends method with the linking length 0.2 times of the mean particle separation. We compute the gravitational potential for each halo particle, and choose the particle with the minimum potential as the center of the halo. We calculate the density $\rho(r)$ in shells with equal logarithmic thickness $\log_{10} \Delta r = 0.1$ from r_{200} inward to about ϵ , a formal force softening limit. Only the halos more massive than 10^4 particles within the virial radius r_{200} are studied here. The density profiles are fitted with Eq. (1) to get the parameter c with an equal logarithmic weighting, i.e.

$$\min \sum_i [\ln \rho(i) - \ln \rho_{NFW}(r_i)]^2, \quad (2)$$

where $\rho(i)$ is the simulation value at the i -th radial bin, and $\rho_{NFW}(r_i)$ is given by Eq. (1) at r_i . We have tested the robustness of our fitting result with a Poisson error weighting and found essentially the same result. Since the Poisson error is negligible compared to the deviation of the fitted profile from the simulation profile, we prefer to use the equal logarithmic weighting. In the fitting, we conservatively set the lower radial limit to 3ϵ . The goodness of the fitting will be characterized by the maximum relative deviation of the simulation $\rho(r_i)$ from the fitted $\rho_{NFW}(r_i)$ in all radial bins $\{i\}$, i.e.

$$\text{dvi}_{\max} = \max\{ |(\rho(r_i) - \rho_{NFW}(r_i)) / \rho_{NFW}(r_i)| \}. \quad (3)$$

We illustrate our measured density profiles in Figure 1 for two CDM models and two SF models. (We do not plot our results for *all* models, because what we have shown is typical and the other models just give qualitatively the same result. This way however saves the space and we will follow this convention throughout the paper. Our results for all

models are summarized in Table 2). The profiles are selected randomly under the condition that their maximum deviations dvi_{max} must be around 0.1, 0.2 and 0.6 respectively in each model. It is important to recall that our fitting is made for $3\epsilon < r < r_{200}$; we plot results for $r < 3\epsilon$ for the sake of discussion in §4. It is interesting to note that the density profiles for $\text{dvi}_{\text{max}} \approx 0.1$ and 0.2 can all be fitted quite satisfactorily with the NFW profile. For the cases of $\text{dvi}_{\text{max}} \approx 0.6$, the NFW profile does not seem to provide a nice description to the simulation data. With a closer look at the figure, we can easily find that there is one feature common to all profiles with $\text{dvi}_{\text{max}} \approx 0.6$: relative to the NFW fit, the halo density is higher than the fitted curve at $r/r_{200} \lesssim 0.03$ (though the simulation result may be underestimated because of the softening at this radius) but lower at $r/r_{200} \gtrsim 0.3$. The shoulder at $r/r_{200} \approx 0.3$ of these profiles can be easily explained as these halos having significant substructures. We have checked the particle distributions of these halos at earlier epoches, and indeed found that they always suffered a violent merging very recently.

With substructure measures, we can quantitatively discuss the relation between the fitting quality and the substructures. Here we use two indicators for the formation history which determines substructures (e.g. Evrard et al. 1993). One is the ratio M_{05}/M , where M is the halo mass and M_{05} is the mass of its largest progenitor at redshift $z = 0.5$. The other is the redshift z_{05} at which the halo’s largest progenitor has reached half of its final mass. The amount of substructures, on average, is a decreasing function of either of these two quantities. In Figure 2, we plot the maximum deviation dvi_{max} versus M_{05}/M or z_{05} for halos in the SCDM and OCDM models. The strong correlations between the dvi_{max} and M_{05}/M or z_{05} confirm that the fitting quality of the NFW profile depends on the formation history, or equivalently the amount of the substructures. The large dispersions seen in the Figure 2 reflect the fact that the both formation history indicators are instant measures at some epoch, but the substructures actually depend on the whole merging history. A better substructure indicator would likely give a much tighter correlation, but quantitatively confirming this statement is beyond the scope of this paper.

We present in Figure 3 the fitted values of c for halos in four models, two SF models and two CDM models. Different symbols are used to indicate the quality of the NFW fit. The circles are for halos with $\text{dvi}_{\text{max}} < 15\%$, the triangles for $15\% < \text{dvi}_{\text{max}} < 30\%$, and the crosses for $\text{dvi}_{\text{max}} > 30\%$. With this classification, it is fair to say that the first subset of halos can be fitted by the NFW profile very well, the second reasonably well, and the third is ill described by the NFW profile because of significant substructures. In order to compare with the NFW results, we plot the NFW prediction c_{NFW} based on their recipe given by Navarro et al. (1997) (the solid lines). The figure assures that the equilibrium halos with $\text{dvi}_{\text{max}} < 15\%$ are in good agreement with the NFW prediction, but the less virialized halos have systematically smaller values of c .

The Probability Distribution Function (PDF) of the fitted c is presented in Figure 4 for the four models. We choose c/c_{NFW} as the abscissa in order to correct for the mass dependence of the parameter c , though this correction for the mass range covered here is actually tiny. The PDF is shown separately for the halos with different amounts of substructure. For each subset of halos, the PDF is fitted by a lognormal function

$$p(c)dc = \frac{1}{\sqrt{2\pi}\sigma_c} \exp - \frac{(\ln c - \ln \bar{c})^2}{2\sigma_c^2} d \ln c. \quad (4)$$

The fitted values of \bar{c} and σ_c are listed in Table 2 for *all* the models. The fitted curves are shown in Figure 4, which indicate that the lognormal function provides an excellent fit to our simulation results of c .

From Table 2 we see that the most virialized halos ($\text{dvi}_{\text{max}} < 15\%$), which are best fitted by the NFW profile, have a mean concentration \bar{c} which also agrees very well with the NFW prediction. The difference between our \bar{c} and the NFW prediction is less than 20% in all models. A similar amount of difference also existed in the original work of NFW between their recipe for c (which is used here) and their simulation result. This agreement between our result and the NFW is not surprising, since both studies are analyzing the equilibrium halos. But considering the vast difference in the simulation methods between the two studies, the agreement is very encouraging and our result gives further supporting evidence to the NFW profile. The less virialized halos (with larger dvi_{max}) have a smaller concentration, i.e. flatter density profile at the center. The mean concentration of the halos with $15\% < \text{dvi}_{\text{max}} < 30\%$ is about 15 percent smaller than that of $\text{dvi}_{\text{max}} < 15\%$ (except for $n = -0.5$).

The dispersion σ_c of $\ln c$ is about 0.2 to 0.35 for the halos with $\text{dvi}_{\text{max}} < 30\%$. The subset of the most virialized halos ($\text{dvi}_{\text{max}} < 15\%$) shows less dispersion with σ_c between 0.17 and 0.27. There appears no clear correlation of the fitting parameters \bar{c} and σ_c with the cosmological parameters or the density power spectrum.

The halos with significant substructures ($\text{dvi}_{\text{max}} > 30\%$) have much smaller concentration and much larger variation in density profile than the more virialized halos. The poor fit of the NFW profile to these halos, however, means that it is not much meaningful to discuss the fitting parameters for this subset. Table 2 indicates that about 35 percent of *all* halos is in this category in the $\Omega_0 = 1$ models. Because the substructure effect is weaker in the $\Omega_0 = 0.3$ models, only about 15 to 20 percent halos have $\text{dvi}_{\text{max}} > 30\%$.

For any simulation study, there exists a concern about the resolution effect, i.e. how much the result is affected by limited resolution. For the present study, such a concern is even enhanced by the recent claims (Fukushige & Makino 1997; Moore et al. 1998) that

$\sim 10^6$ particles are necessary to correctly sample the density profile of a single halo. It is usually a tough task to quantify the resolution effect, but fortunately, our newly available high-resolution halos can serve this purpose. In an ongoing project, we have developed a modified P³M algorithm which adopts nested grids to simulate single halos (For clarity, we will call this simulation as ‘halo simulation’, and the simulations we described in §2 as ‘cosmological simulation’). We are using this code to simulate fifteen halos with $\sim 2 \times 10^6$ particles ($\sim 10^6$ particles end up within the virial radius). Each halo is evolved by 10000 time steps with a force resolution much higher than that of the present paper. A Detailed discussion of the project will be published elsewhere (Jing & Suto, 2000). Of the fifteen halos, five are randomly selected from the LCDM halos of the present paper. As of this writing, we have finished simulating two of them. One halo has significant substructures with $\text{dvi}_{\text{max}} = 0.63$, and the other is much more virialized with $\text{dvi}_{\text{max}} = 0.21$. The density profiles of these two high-resolution halos are plotted in Figure 5. For radius larger the resolution limit (3ϵ) defined in this paper, the new density profiles are in excellent agreement with those used in the present paper. It is more gratifying to see that even fine substructure features of the density profiles match very well in the both simulations, with $\text{dvi}_{\text{max}} = 0.69$ and 0.18 respectively for the high-resolution halos. We can therefore safely conclude that our measured quantities are robust and are little affected by the simulation resolution. It is worth pointing out that this conclusion is not inconsistent with the studies of Fukushige & Makino (1997) and Moore et al. (1998), since they declare that $\sim 10^6$ particles are needed for studying the core region with $r/r_{200} \lesssim 0.01$ while the present work is studying an outer region with $r/r_{200} \gtrsim 0.03$. In fact, our result of the virialized halo in Fig. 5 supports their claims for the core region, and the resolution tests conducted by Moore et al. (1998) indicated as well that $\sim 10^4$ particles are sufficient for studying the density profile at $r/r_{200} \gtrsim 0.03$. Since the survival time of substructures is much shorter in the core region than in outer region, the scales relevant to the present study are $r/r_{200} \sim 0.1$ (see Fig. 1), therefore the simulations used here are adequate for the present work. Fig. 5 also implies that the resolution limit we defined is slightly too conservative.

4. Conclusion and further discussion

In this paper we have measured the density profiles for massive halos in a large set of high-resolution cosmological simulations. Four scale-free models and three representative CDM models are studied. We selected all halos with more than 10^4 particles within the virial radius and fitted their density profiles with the NFW profile. We found,

- The quality of the NFW profile fitting depends on if the halo is in equilibrium.

Substructures degrade the fitting quality, as expected, because the NFW profile was found for equilibrium halos.

- We use the maximum deviation dvi_{max} of the simulation density profile from the fitted NFW profile as an indicator for the fitting quality. In the Einstein de Sitter universes, about 15 percent of halos have $\text{dvi}_{\text{max}} < 0.15$ and 50 percent have $0.15 < \text{dvi}_{\text{max}} < 0.30$. In the low density models, these percentages are higher, because the substructure effect is weaker. These numbers show that the NFW profile provides a good description for most of DM halos ($\gtrsim 70\%$).
- For the halos which can be fitted by the NFW profile, there is a considerable amount of dispersion in the parameter c . The lognormal function Eq. (4) provides a very good fit to the distribution of c . Our fitted values for \bar{c} and σ_c are listed in Table 2. The mean value \bar{c} of the most virialized halos ($\text{dvi}_{\text{max}} < 0.15$) is in good agreement with the NFW prediction. The less virialized halos ($0.15 < \text{dvi}_{\text{max}} < 0.30$, which can still be reasonably fitted by the NFW profile) have a smaller concentration with \bar{c} about 15 percent smaller than that of the most virialized ones. The dispersion σ_c is around 0.25, with the virialized halos being slightly less dispersive.

In a word, our results are in good agreement with the results of NFW for the most virialized halos, but we extend the discussion of the density profiles to less virialized halos which may account for most of the halos in number. The new result of this work is that we have quantified how much halos can really be fitted by the NFW profile and that we have derived the important quantity, the probability distribution function of the concentration parameter c .

The NFW profile has been used to analytically model the formation of disk galaxies in the framework of hierarchical clustering (Dalcanton, Spergel & Summers 1997, Mo Mao & White 1998, Mao & Mo 1998, van den Bosch 1998). In such a approach, the Press-Schechter formalism is usually used to calculate the abundance of halos, which means that almost all halos, in equilibrium or with substructures, have been considered. Since our results indicate that most of the halos can be reasonably fitted by the NFW profile, these approaches are valid. But for the bulk of halos, a slightly smaller concentration c is preferred over the value given by NFW that is for equilibrium halos. The dispersion of c should also be properly taken into account to survey various properties of disk galaxies.

Our results would also be important for properly interpreting many cosmological observations which are closely related to the density profile of halos. The extragalactic objects (say, clusters of galaxies, galaxies) that are observed are not guaranteed to be at the equilibrium state. Our results, i.e. a smaller concentration c for less virialized halos and

the large dispersion of c , can alleviate the conflicts recently found between the observed rotation curves of galaxies, the observed core radius of galaxies and clusters, and the predictions based on the NFW profile (Makino Sasaki & Suto 1998, MCGaugh & De Blok 1998, Navarro 1998).

Kravtsov et al. (1998) discussed the variation of density profiles in a way very different from our present work. They compared the rotation curves of galactic CDM (or ν CDM) halos with a sample of observed rotation curves, and claimed a good agreement. Comparing with the NFW density profile, however, they found that their simulated density profiles, while having a large dispersion, are significantly flatter (density about 5 to 10 times lower) at $r \approx 0.01r_{200}$. Our result does not seem to agree with their result. Although we conservatively set the force softening to $0.03r_{200}$, the fitted NFW profile follows very well our simulation result down to $r \approx 0.01r_{200}$ (see Fig. 1). We could only expect that the force softening, if any, would have flattened our simulated profile at $r = 0.01r_{200}$. Of course we note that our halos in the CDM models are at cluster scale, but those of Kravtsov et al. are at galactic scale. It appears unlikely that the mass difference can explain the difference in the density profiles, because none of our SF models ($n = -0.5$ to -2) shows significantly flatter density profile than the NFW result at the core region (also see the results of NFW for galactic halos). We think that the discrepancy can only be explained by the differences in the simulation methods and/or in the ways to define the resolution limit. It is interesting to note that the previous studies with the tree codes (NFW, Moore et al. 1998) and with GRAPE (Fukushige & Makino 1997) and the present work with the P^3M method have produced very consistent results at the central core if an account is taken for the resolution limits.

It would be also important to point out that we could not address the important problem that density profile might be significantly steeper than r^{-1} in the very inner region of the halos (Fukushige & Makino 1997; Moore et al. 1998) because the resolution of our current simulations is still limited. We are running a project to simulate many halos with higher mass resolution ($\sim 10^6$ particles within r_{200}) and force resolution ($\epsilon < 0.002r_{200}$). We shall report these results in a future paper (Jing & Suto, 2000).

I would like to thank Gus Evrard, Yasushi Suto and Simon White for helpful comments and discussion, and the JSPS foundation for a postdoctoral fellowship. The simulations were carried out on VPP/16R and VX/4R at the Astronomical Data Analysis Center of the National Astronomical Observatory, Japan.

REFERENCES

- Carlberg, R. G., Morris, S. L., Yee, H. K. C. & Ellingson, E. 1997, ApJ, 479, L19
- Carlberg, R. G., et al. 1997, ApJ, 485, L13
- Dalcanton, J. J., Spergel, D. N. & Summers, F. J. 1997, ApJ, 482, 659
- Evrard, A. E., Mohr, J. J., Fabricant, D. G., & Geller, M. J. 1993, ApJ, 419, L9
- Jing, Y. P. 1998a, ApJ, 503, L9
- Jing, Y. P. 1998b, in proceedings of Evolution of Large-Scale Structure: From Recombination to Garching, in press
- Jing, Y. P. 1999, ApJ, 515, L45
- Jing, Y. P. & Suto, Y. 1998, ApJ, 494, L5
- Jing, Y. P. & Suto, Y. 2000, ApJ(Letters), Feb. issue
- Jing, Y. P., Mo, H. J., Börner, G. & Fang, L. Z. 1995, MNRAS, 276, 417
- Kravtsov, A. V., Klypin, A. A., Bullock, J. S. & Primack, J. R. 1998, ApJ, 502, 48
- Makino, N., Sasaki, S. & Suto, Y. 1998, ApJ, 497, 555
- Mao, S. & Mo, H. J. 1998, MNRAS, 296, 847
- McGaugh, S. S. & De Blok, W. J. G. 1998, ApJ, 499, 41
- Mo, H. J., Mao, S. & White, S. D. M. 1998, MNRAS, 295, 319
- Moore, B., Governato, F., Quinn, T., Stadel, J. & Lake, G. 1998, ApJ, 499, L5
- Navarro, J. F. 1998, astro-ph/9807084
- Navarro, J. F., Frenk, C. S. & White, S. D. M. 1995, MNRAS, 275, 720
- Navarro, J. F., Frenk, C. S. & White, S. D. M. 1996, ApJ, 462, 563
- Navarro, J. F., Frenk, C. S. & White, S. D. M. 1997, ApJ, 490, 493
- Persic, M., Salucci, P. & Stel, F. 1996, MNRAS, 281, 27
- Steidel, C. C., Adelberger, K. L., Dickinson, M., Giavalisco, M., Pettini, M., Kellogg, M., 1998, ApJ, 492, 428

Thomas, P. A., et al. 1998, MNRAS, 296, 1061

Tyson, J.A., Kochanski, G.P., Dellantonio, I.P., 1998, ApJ, 498, L107

Van Den Bosch, F. C. 1998, ApJ, 507, 601

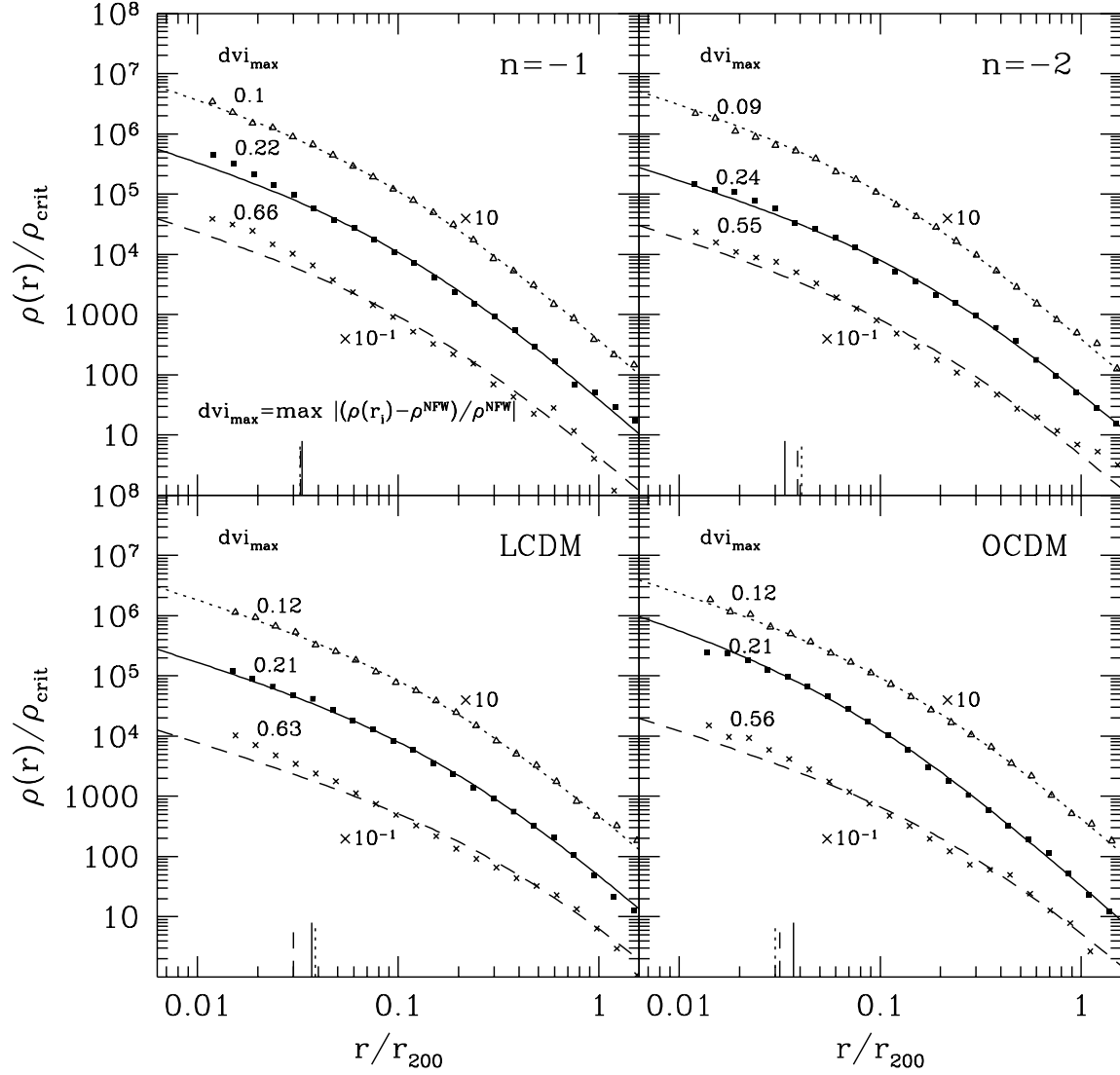


Fig. 1.— Illustration of halo density profiles in different cosmological models. Three halos are randomly selected in each model with the maximum deviation dvi_{\max} about 0.1, 0.2, 0.6 respectively. The exact value of dvi_{\max} is labeled with a number below dvi_{\max} . The profiles with the smallest and the largest dvi_{\max} are shifted by one magnitude vertically, as also indicated in the figure. The long ticks at the bottom of each panel mark the lower radius limits used for the NFW fitting.

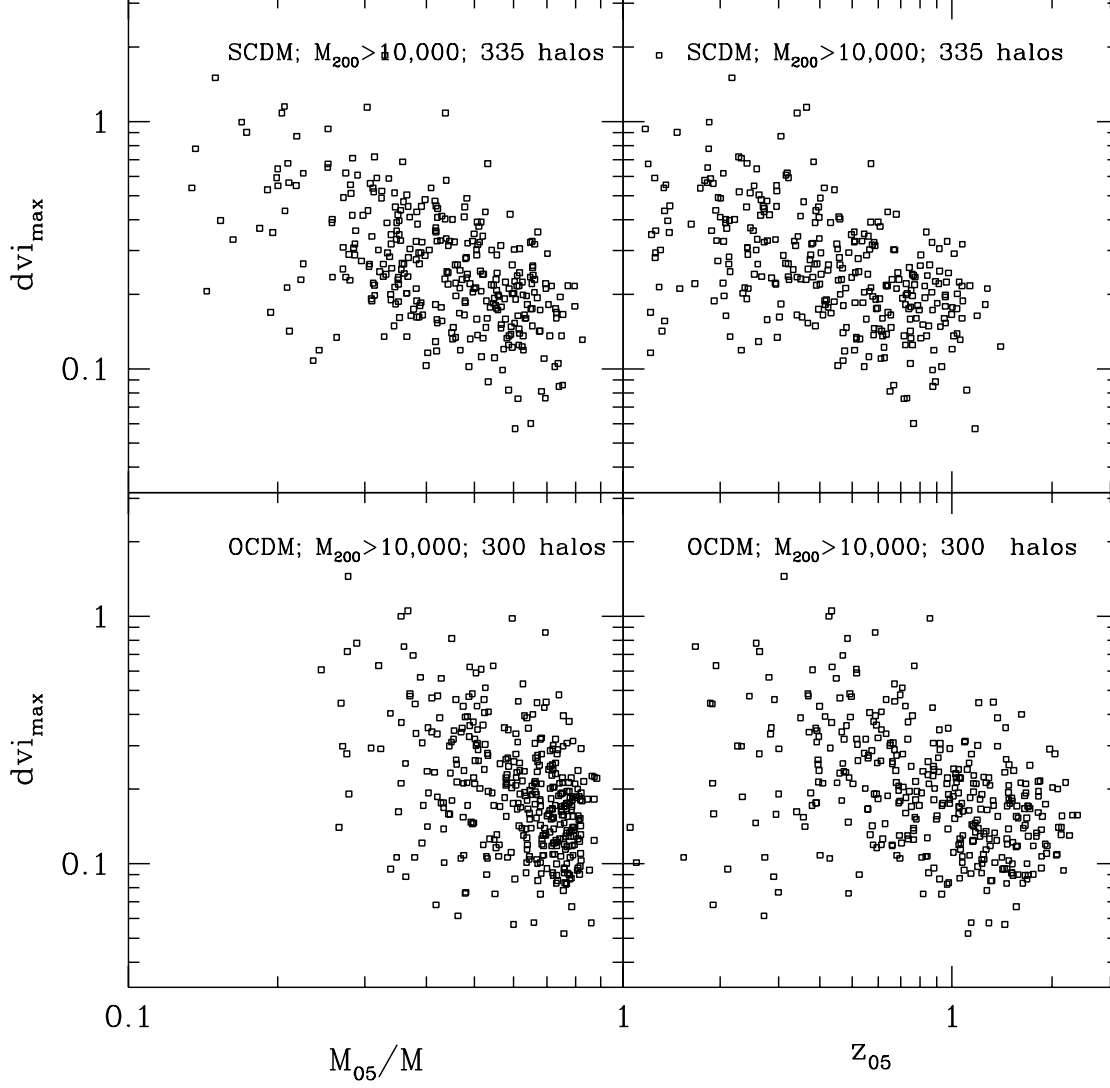


Fig. 2.— The maximum deviation versus the formation history indicators M_{05}/M or z_{05} .

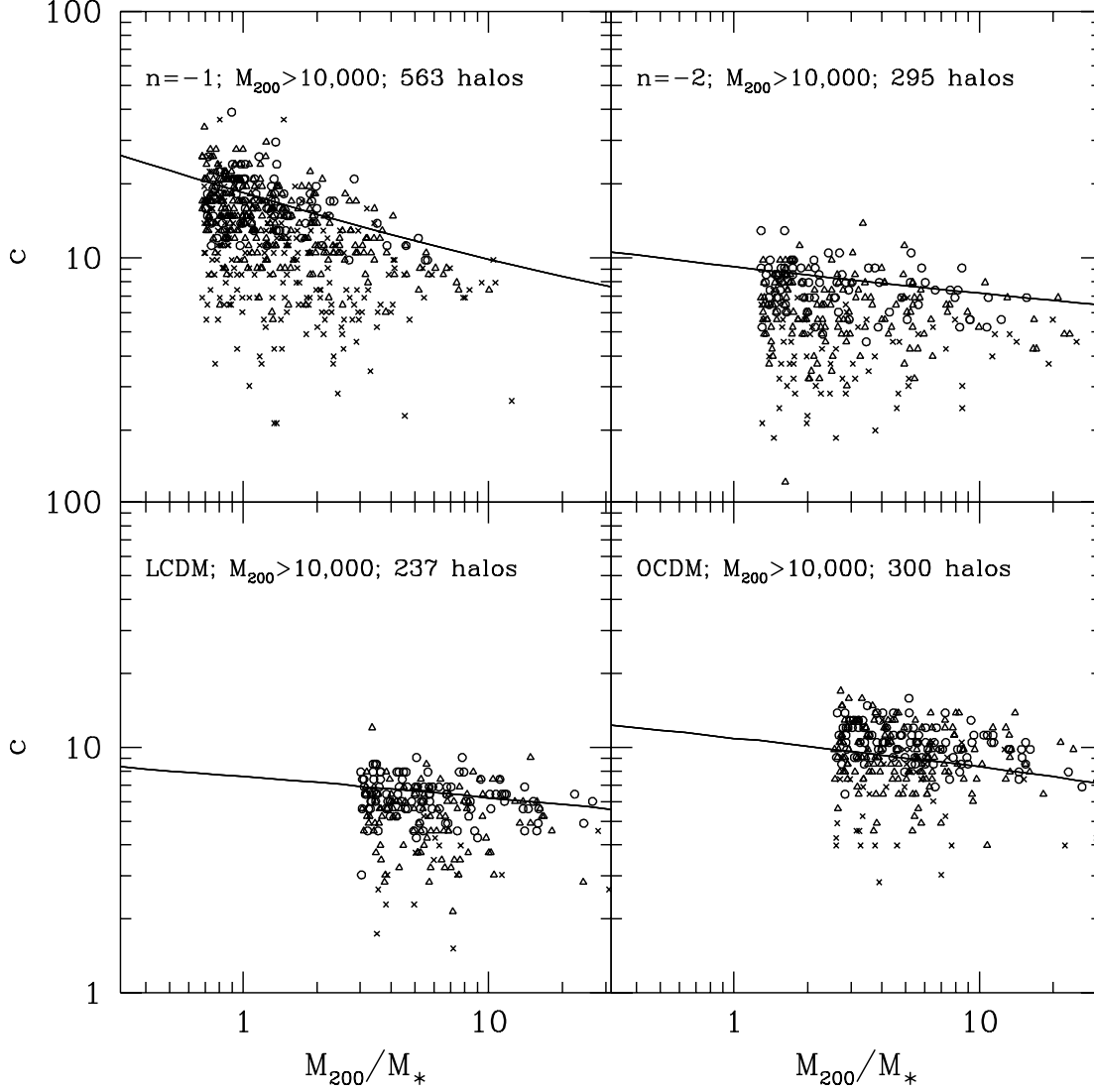


Fig. 3.— The concentration factor c is shown for four cosmological models as a function of the halo mass M_{200} . Different symbols are used to denote the quality of the NFW profile fit, with the circles for $dvi_{\max} < 0.15$, the triangles for $0.15 < dvi_{\max} < 0.30$, and the crosses for $dvi_{\max} > 0.30$. The lines are the prediction based on the NFW's recipe.

Fig.4a

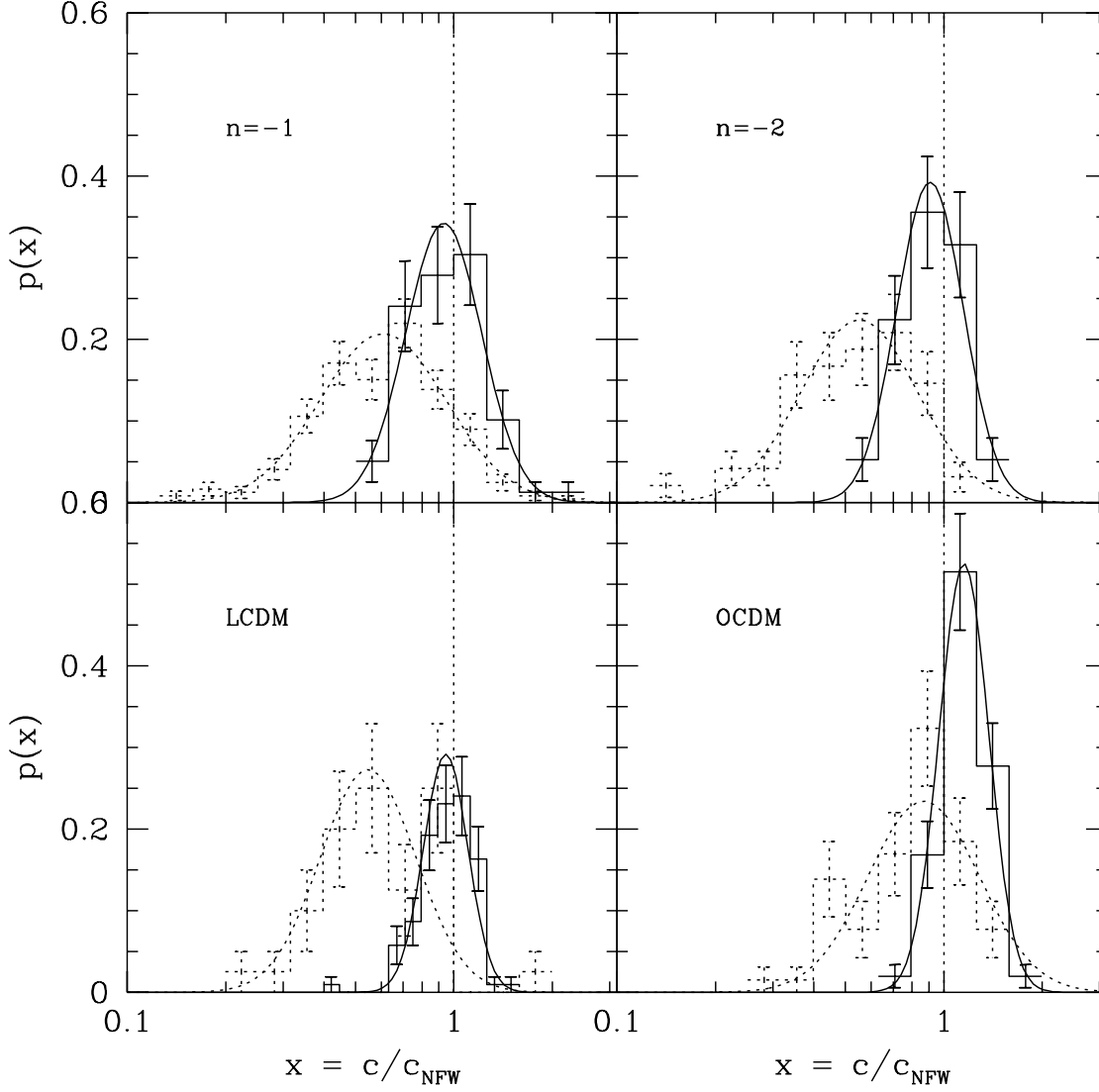
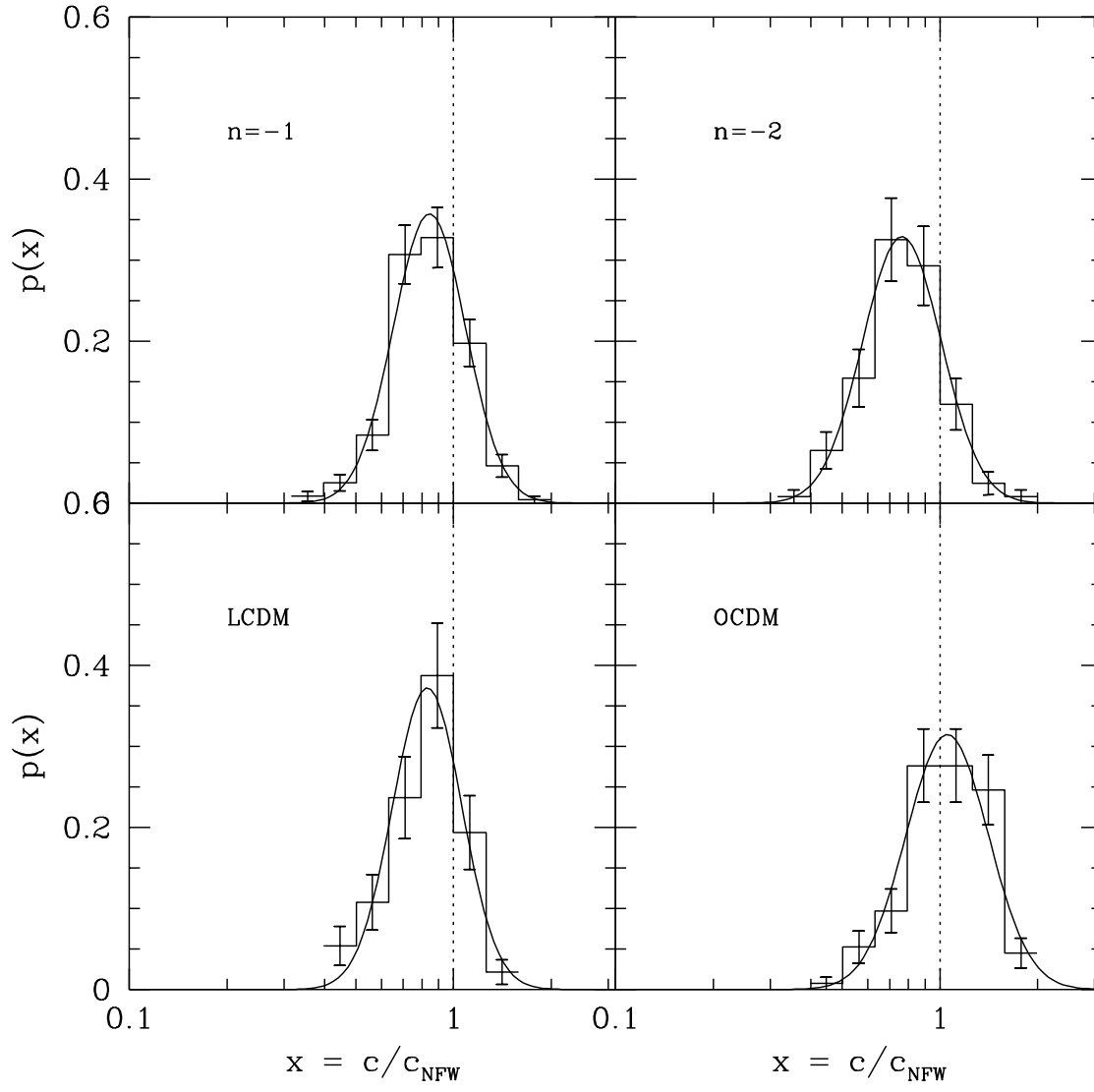


Fig. 4.— The probability distribution function of the concentration parameter c (histograms), which can be nicely fitted by lognormal distributions (smooth lines). **a).** The solid lines are for the halos with $dv_{i,\text{max}} < 0.15$ and the dotted ones for $dv_{i,\text{max}} > 0.30$; **b).** for $0.15 < dv_{i,\text{max}} < 0.30$.

Fig.4b



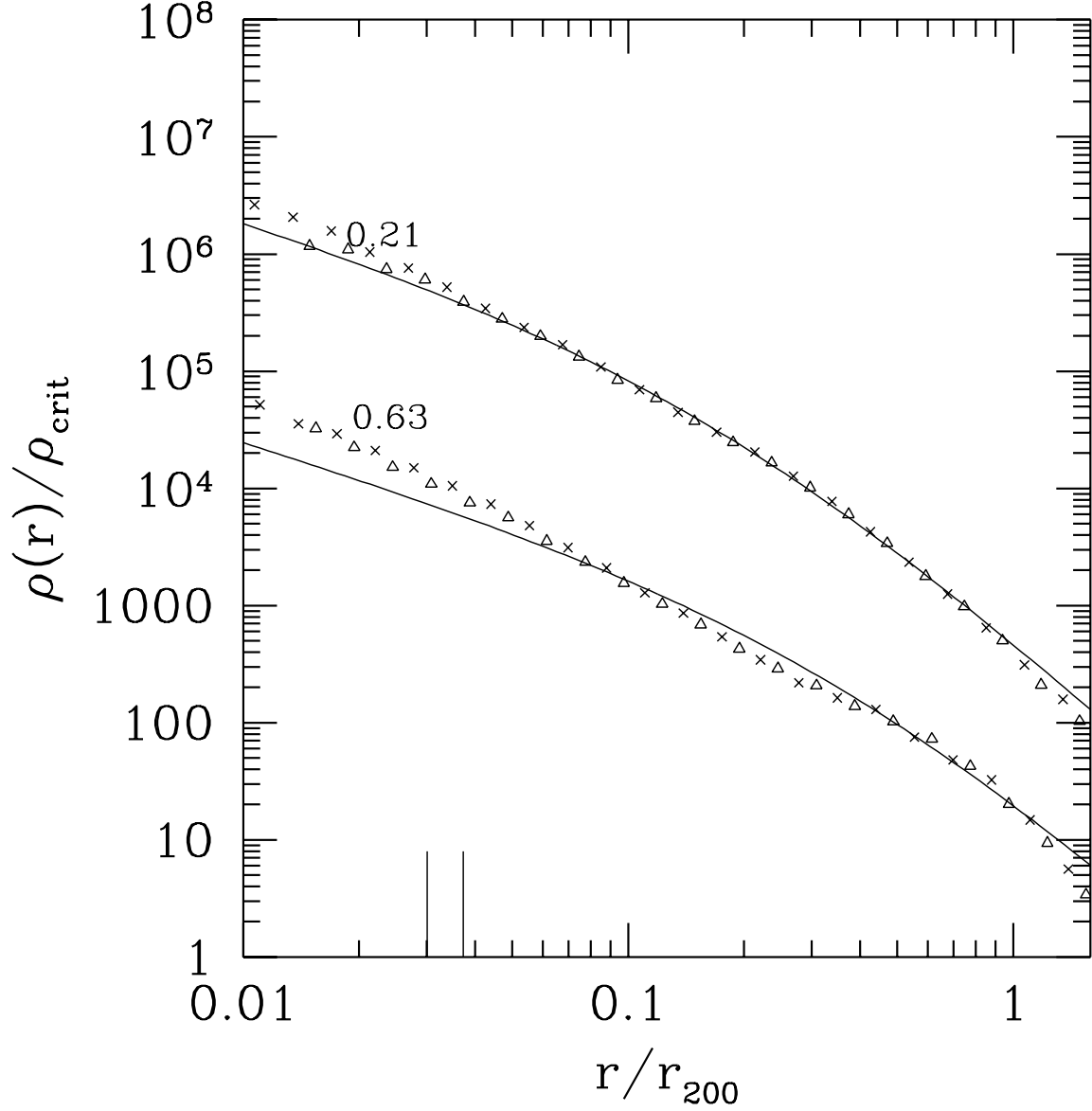


Fig. 5.— The density profiles of the two halos in the LCDM model that are resimulated with a higher resolution, $\sim 10^6$ particles within the virial radius. The crosses show the result of these high resolution halo simulations, which should be compared with the profiles used for the present analysis (triangles; lower resolution). It is gratifying to see that the profiles of the different simulations agree very well for scales larger than the resolution limit (long ticks). The upper profiles have been vertically shifted up by a factor 10.

Table 1. Simulations of 256^3 particles

Model	Ω_0	λ_0	Γ or n ^a	σ_8 or M_* ^b	L ^c	Num. ^d
SCDM	1.0	0.0	0.5	0.85	100	3
LCDM	0.3	0.0	0.25	1.0	100	3
OCDM	0.3	0.7	0.20	1.0	100	3
SF1	1.0	0.0	−0.5	18882		3
SF2	1.0	0.0	−1.0	14827		3
SF3	1.0	0.0	−1.5	8832		3
SF4	1.0	0.0	−2.0	7834		3

^aThe shape of the linear power spectrum. The CDM models are specified by Γ , and the scale-free models by n

^bThe amplitude of the linear power spectrum at the final epoch. The scale-free models are specified by M_* and the CDM models by σ_8 . M_* is in units of the particle mass

^cIn $h^{-1}\text{Mpc}$

^dNumber of independent realizations

Table 2. Number of halos N_h and the fitting results of \bar{c} and σ_c for a fixed range dvi_{max} ^a

Model	$0 < \text{dvi}_{\text{max}} < 0.15$			$0.15 < \text{dvi}_{\text{max}} < 0.30$			$0.0 < \text{dvi}_{\text{max}} < 0.30$			$\text{dvi}_{\text{max}} > 0.30$		
$n = -0.5$	70	0.80	0.21	257	0.84	0.32	327	0.84	0.30	352	0.65	0.50
$n = -1$	79	0.93	0.27	238	0.84	0.26	317	0.86	0.26	246	0.61	0.44
$n = -1.5$	84	0.96	0.18	182	0.79	0.30	266	0.84	0.28	156	0.59	0.38
$n = -2$	76	0.91	0.23	123	0.76	0.28	199	0.81	0.27	96	0.55	0.41
SCDM	57	0.99	0.18	159	0.90	0.20	216	0.92	0.20	119	0.63	0.28
LCDM	104	0.95	0.17	93	0.83	0.25	197	0.90	0.20	40	0.55	0.33
OCDM	101	1.25	0.17	134	1.05	0.29	235	1.10	0.23	65	0.87	0.39

^aThree numbers, for example 70 0.80 0.21, in each column are N_h , \bar{c} , and σ_c respectively